

1 **Characterization of satellite based proxies for estimating nucleation mode**
2 **particles over South Africa**

3
4
5 **A.-M. Sundström¹, A. Nikandrova¹, K. Atlaskina¹, T. Nieminen¹, V. Vakkari^{2,1}, L.**
6 **Laakso^{2,3}, J.P. Beukes³, A. Arola⁴, P.G. van Zyl³, M. Josipovic³, A.D. Venter³, K.**
7 **Jaars³, J.J. Pienaar³, S. Piketh³, A. Wiedensohler⁵, E.K. Chiloane^{3,6}, G. de**
8 **Leeuw², and M. Kulmala¹**

9 [1]{Department of Physics, University of Helsinki, Helsinki, Finland}

10 [2]{ Finnish Meteorological Institute, Helsinki, Finland. }

11 [3]{Unit for Environmental Science and Management, North-West University, Potchefstroom,
12 South Africa}

13 [4] {Finnish Meteorological Institute, Kuopio, Finland. }

14 [5] {Leibniz Institute for Tropospheric Research, Leipzig, Germany}

15 [6] {Eskom Holdings SOC Ltd, Sustainability Division, South Africa}

16
17 **Abstract**

18 Proxies for estimating nucleation mode number concentrations and further simplification for
19 their use with satellite data have been presented in Kulmala et al. (2011). In this paper we
20 discuss the underlying assumptions for these simplifications and evaluate the resulting
21 proxies over an area in South Africa based on comparison with a suite of ground-based
22 measurements available from four different stations. The proxies are formulated in terms of
23 sources (concentrations of precursor gases (NO₂ and SO₂), and UV-B radiation intensity near
24 the surface), and a sink term related to removal of the precursor gases due to condensation on
25 pre-existing aerosols. A-Train satellite data are used as input to compute proxies. Both the
26 input data and the resulting proxies are compared with those obtained from ground-based
27 measurements. In particular a detailed study is presented on the substitution of the local
28 condensation sink (CS) with satellite aerosol optical depth (AOD) which is a column-
29 integrated parameter. One of the main factors affecting the disagreement between CS and
30 AOD is the presence of elevated aerosol layers. Overall, the correlation between proxies

1 calculated from the in situ data and observed nucleation mode particle number concentrations
2 (N_{nuc}) remained low. At the time of the satellite overpass (13-14 LT) the highest correlation is
3 observed for SO_2/CS ($R^2=0.2$). However, when the proxies are calculated using satellite data,
4 only NO_2/AOD showed some correlation with N_{nuc} ($R^2=0.2$). This can be explained by the
5 relatively high uncertainties related especially to the satellite SO_2 columns and by the positive
6 correlation that is observed between the ground-based SO_2 and NO_2 concentrations. In fact,
7 results show that the satellite NO_2 columns compare better with in situ SO_2 concentration
8 than the satellite SO_2 column. Despite the high uncertainties related to the proxies calculated
9 using satellite data, the proxies calculated from the in situ data did not predict significantly
10 better N_{nuc} . Hence, overall improvements in the formulation of the proxies are needed.

11

12 **1 Introduction**

13 Aerosol particles are key constituents in the Earth-Atmosphere system that can alter climate
14 through their direct and indirect effects on the Earth's radiation budget. Aerosols affect the
15 radiation budget directly by scattering and absorbing solar radiation, and indirectly by acting
16 as cloud condensation nuclei or ice nuclei and modifying clouds' radiative properties and
17 lifetimes. However, the quantification of the aerosol effects on climate is very complex and
18 large uncertainties still exist due to the high spatial and temporal variability of aerosol mass
19 and particle number concentrations (e.g. IPCC, 2013). Besides the climatic effects, aerosols
20 affect human life by reducing the air quality and visibility as well as affecting human health
21 especially in urban areas. Particulate air pollution has been associated with adverse
22 cardiovascular and pulmonary diseases, and even with rises in the numbers of deaths among
23 older people (e.g. Seaton et al., 1995 Uttel et al., 2000, Schnelle-Kreis, 2009).

24 Primary aerosol particles are emitted directly into the atmosphere; e.g. sea spray aerosol,
25 desert dust, aerosol generated from biomass burning and fossil fuel combustion. Secondary
26 particles are formed from precursor gases through gas-to-particle conversion. The formation
27 of new particles is strongly connected to the presence of sulphuric acid and other vapours of
28 very low volatility, as well as the magnitude of solar radiation (e.g. Kulmala et al., 2008,
29 Kulmala et al., 2005). On the other hand pre-existing aerosol particles act as a sink for the
30 vapours inhibiting new aerosol formation (e.g. Kulmala et al, 2008). These new nanometer-
31 size aerosol particles grow through condensation and coagulation to sizes where they may act

1 as cloud condensation nuclei (particle diameter $D_p \sim 50$ nm) or where they are large enough
2 ($D_p > \sim 100$ nm) to scatter solar radiation and thus affect the Earth's radiation budget.

3 Several studies have shown that nucleation occurs frequently in the continental boundary
4 layer and free troposphere from clean to polluted environments (Kulmala et al., 2004,
5 Kulmala et al. 2008 and references therein). Laakso et al. (2008) and Vakkari et al. (2011)
6 have studied new particle formation over moderately polluted savannah ecosystems in South
7 Africa and found that nucleation takes place in the boundary layer almost every sunny day
8 throughout the year with a frequency of as high as 69% of all analysed days (Vakkari et al.
9 (2011)). Hirsikko et al. (2012) extended the studies in South Africa to a polluted
10 measurement site and found an even higher frequency for the nucleation event days (86%),
11 which is among the highest event frequencies reported in the literature so far. Hirsikko et al.
12 (2013) also studied the causes for two or three consecutive daytime nucleation events,
13 followed by subsequent particle growth during the same day. They concluded e.g. that the
14 multiple events were associated with SO_2 rich air from industrial sources.

15 Satellite instruments have been providing global observations of the Earth's atmosphere for
16 three decades (e.g. Lee et al., 2009, Kokhanovsky and de Leeuw, 2009, Burrows et al., 2011).
17 Information about the spatial distribution of aerosols and trace gases can be obtained from
18 multiple instruments with various temporal and spatial resolution and coverage. Passive
19 remote sensing instruments such as NASA's Ozone Monitoring Instrument (OMI) onboard
20 the AURA platform or the Moderate Resolution Imaging Spectroradiometer (MODIS)
21 onboard the Terra and Aqua platforms use solar radiation to detect either trace gases or
22 aerosol and cloud properties. Trace gas remote sensing techniques using OMI are based on
23 the trace gas absorption features in the UV-region (wavelength $\lambda \sim 200$ -400 nm), whereas the
24 remote sensing of aerosol particles is mainly based on measurements in the UV/visible and
25 near infrared regions ($\lambda \sim 500$ -2000 nm). Since the aerosol measurements utilize only the
26 optically active size range of the solar spectrum, the detectable aerosol sizes are limited to
27 particles with diameters greater than about 100 nm. Nucleation mode particles (smaller than
28 about 25-30 nm in diameter), therefore, cannot be detected directly using satellite instruments.
29 In 2011 Kulmala et al. introduced proxies, i.e. parameterizations for estimating the number
30 concentrations of nucleation mode (N_{nuc}) simplified for the use with satellite data. These
31 simplifications were made assuming that in situ parameters could be replaced with satellite-
32 based observations. Their study was the first attempt to estimate the global nucleation mode
33 aerosol concentrations using data derived from satellite measurements. The proxies were

1 defined in terms of sources and sinks. The nucleation source terms consist of precursor gas
2 column densities (NO_2 or SO_2) and UV-radiation intensity near the surface (all from OMI as
3 opposed to in situ data in the initial proxies) whereas the sink term, i.e. the condensation sink
4 in the original proxy formulation related to the aerosol surface area concentration is assumed
5 to be proportional to the aerosol optical depth (AOD, from MODIS). More recently Crippa et
6 al. (2013) formulated a new proxy algorithm for ultrafine particle number concentrations
7 based on satellite-derived parameters. They used multivariate linear regression approach to
8 derive the proxy, where the source terms consisted of SO_2 , UV (from OMI), and NH_3 (from
9 Tropospheric Emission Spectrometer, TES). The sink term was formulated using MODIS
10 (collection 5.0) AOD and the Ångström exponent, which expresses the spectral dependence
11 of AOD on the wavelength. However, there are issues with the Ångström coefficient (e.g.
12 Mielonen et al., 2011), and thus this parameter is no longer included in the most recent
13 MODIS collection 6.0 land parameters (Levy et al., 2013).

14 In this work we evaluate the simplifications and underlying assumptions of the method
15 introduced in Kulmala et al. (2011) to estimate the number concentration of nucleation mode
16 particles from satellite-derived data. The study area is the north-eastern part of South Africa
17 (25-28S, 25.5 -30.5E, Figure 1.). Even though the area is not very large, it comprises lots of
18 contrasts from the emission point of view; the cities of Johannesburg and Pretoria, as well as
19 highly industrialized areas especially east from the cities, versus a very clean background in
20 the western part of the study area. The study period considered is Jan 2007- Dec 2010. There
21 are also four different measurement stations located within the region of interest, where
22 observations of various in situ parameters were available.

23 This work comprises of two parts:

- 24 1) A detailed investigation of replacing the condensation sink (CS, defined below in Eq.
25 8), a local parameter evaluated from in situ observations, with the AOD, a column-
26 integrated aerosol property available from satellite.
- 27 2) The estimation of how well satellite data can be used to compute proxies for
28 nucleation mode particle number concentrations. This comprises the analysis of both
29 the satellite- and in situ-based proxy components and the proxies, as well as the
30 comparison of the proxies with the measured concentration of nucleation mode
31 particles. The influence of the uncertainties in the satellite-derived quantities on the
32 proxy is also evaluated.

1 2 Data

2 In this study, a variety of data was used from satellite instruments and ground-based stations
3 (see Table 1 for a summary). Satellite data used originate from NASA's Afternoon-Train (A-
4 Train) constellation. The A-Train constellation consists of seven satellites that are on a same
5 polar-orbiting track and follow each other closely enabling near-simultaneous observations of
6 a variety of atmospheric parameters. The equatorial overpass for the A-Train satellites is
7 around 1:30 p.m. local time. In this study we use OMI Level 2 products, i.e. the NO₂
8 tropospheric column (Bucsela et al., 2013), the SO₂ planetary boundary layer (PBL) product
9 (Krotkov et al., 2006, Krotkov et al., 2008), and the 310 nm irradiance (UV-B) at surface at
10 local noon (Tanskanen et al., 2006). It is noted that the OMI SO₂ PBL product describes the
11 SO₂ concentration integrated over the whole atmospheric column, and PBL refers to the a
12 priori profile assumed in the retrieval of this product. The OMI L2 products are provided with
13 a nominal spatial resolution of 13 x 24 km². For the current study they were re-gridded
14 onto a 3 km x 3 km geographical grid as in Fioletov et al. (2011). In this way the effective
15 spatial resolution could be increased despite that the instrument resolution is coarser than the
16 grid. For NO₂ and SO₂ only those observations were used where the (radiative) cloud
17 fraction was below 20%.

18 According to Lamsal et al. (2014), and references therein, the uncertainty in the OMI NO₂
19 tropospheric column concentrations is about $0.75 \cdot 10^{15}$ molec./cm², whereas Krotkov et al.
20 (2008) report that the SO₂ PBL product could be associated with noise as high as 1.5 DU.
21 However averaging the SO₂ columns over longer a period and/or over a larger spatial area
22 could reduce the noise to 0.3-0.6 DU. For OMI UV-B irradiance the relative uncertainty is on
23 average 7%, but could be higher e.g. due to some episodic aerosol plumes (Tanskanen et al.,
24 2006).

25 The AOD used in this study is the MODIS Aqua collection 6.0 AOD product at 3 km spatial
26 resolution (Levy et al., 2013). The relative uncertainty for the MODIS AOD over land is
27 reported as 0.05+15%. For selected cases also vertical aerosol extinction profiles from the
28 Cloud-Aerosol Lidar and Infrared Pathfinder Satellite Observation (CALIPSO) (Winker et al.,
29 2007) are used.

30 The in situ data used in this study are collected at four different stations in South Africa:
31 Elandsfontein (ELA), Marikana (MAR), Botsalano (BOT), and Welgegend (WEL). All of
32 these stations are located in the north eastern part of the country shown in Fig. 1. Depending

1 on the station, the measured parameters included e.g. particle size distribution, extinction
2 coefficient and trace gas concentrations. More detailed description of the in situ
3 measurements can be found e.g. in Kulmala et al. (2011), Beukes et al. (2014), Hirsikko et al.
4 (2012), Venter et al. (2012), Vakkari et al. (2011), Laakso et al. (2012), and Vakkari et al.
5 (2013). Also data from the Aerosol Robotic Network (AERONET,
6 <http://aeronet.gsfc.nasa.gov>, Holben et al., 1998) at the Elandsfontein station is used.
7 AERONET is a global ground-based sunphotometer network, providing observations of
8 aerosol optical, microphysical, and radiative properties that are available in a public domain.
9 The aerosol optical properties in the total atmospheric column are derived from the direct and
10 diffuse solar radiation measured by the Cimel sunphotometers.

11

12 **3 Proxies**

13 Regional scale nucleation is associated with photochemistry, and typically occurs over a
14 spatial scale of hundreds of kilometres (Kulmala et al., 2011; and references therein). The
15 number concentration of nucleation mode particles on a regional scale can be estimated from
16 consideration of the sources, i.e. precursor gas concentrations such as sulphur dioxide (SO₂),
17 the UV-radiation intensity needed to initiate the photochemical reaction, and a sink term
18 which reduces the nucleation potential by removing precursor gases (Petäjä et al., 2009):

$$19 \quad P_{N_{nuc,regional}} = \frac{UV \cdot [SO_2]}{CS^2} \quad (1)$$

20 Primary emissions occur in the vicinity of local sources such as industrial or urban areas. For
21 nucleation from primary emissions two proxies are defined as (Kulmala et al., (2011)):

$$22 \quad P_{N_{nuc,prim.}} = \frac{[NO_2]}{CS}, \quad (2)$$

$$23 \quad P_{N_{nuc,prim.}} = \frac{[SO_2]}{CS}, \quad (3)$$

24 In each of the proxies the source terms are estimated from the satellite measurements by
25 replacing the SO₂ and NO₂ concentrations at the surface with the column densities from the
26 satellite. The amount of global UV radiation is also available from satellite measurements e.g.
27 as a local noon irradiance at 310 nm wavelength (UV-B-radiation) at the surface. For the sink
28 parameter (CS), Kulmala et al. (2011) proposed to use the AOD which describes the total

1 aerosol extinction in the atmospheric column. The relation between the CS and the AOD will
 2 be discussed in the following section. By replacing CS with AOD the simplified proxy for
 3 using satellite data for primary nucleation becomes:

$$4 \quad P_{N_{nuc}}^{Sat.} = \frac{[NO_2]_{column}}{AOD} \quad (4)$$

$$5 \quad P_{N_{nuc}}^{Sat.} = \frac{[SO_2]_{column}}{AOD} \quad (5)$$

6 For regional nucleation the proxy expressed in terms of satellite data becomes

$$7 \quad P_{N_{nuc}}^{Sat.} = \frac{UV[SO_2]_{column}}{AOD^2} \quad (6)$$

8 In addition we also considered

$$9 \quad P_{N_{nuc}}^{Sat.} = \frac{UV}{AOD^2} \quad (7)$$

10 as a potential proxy for the number concentration of nucleation mode particles.

11

12 **3.1 Condensation sink and aerosol extinction**

13

14 As indicated in the previous section, Kulmala et al. (2011) proposed AOD as a substitute for
 15 CS. Both parameters are also roughly proportional to the aerosol surface area distribution.
 16 According to e.g. Lehtinen et al. (2003) the condensation sink is defined as

$$17 \quad CS = 2\pi\rho_{diff} \int_0^{\infty} D_p \beta_M(D_p) n(D_p) dD_p \quad (8)$$

18 , where D_p is the particle radius, $n(D_p)$ is the particle number size distribution function, ρ_{diff} is
 19 the diffusion coefficient, and $\beta_M(D_p)$ is the transitional correction factor.

20 Aerosol optical depth describes quantitatively the column-integrated extinction of solar light
 21 caused by atmospheric aerosols and it is one of the standard aerosol parameters that is
 22 retrieved from the satellite radiance observations. At a height z and for a wavelength λ the
 23 aerosol extinction is defined as

$$1 \quad \sigma_{ext,z,\lambda} = \frac{1}{4} \pi \int_0^{\infty} Q_{ext}(\lambda, D_p, m) D_p^2 n(D_p) dD_p, \quad (9)$$

2 where Q_{ext} is the extinction efficiency describing aerosols ability to scatter and absorb solar
3 light. At a fixed wavelength the extinction efficiency is a complex function of aerosol size
4 and complex refractive index m (which in turn depends on the aerosol particle composition).
5 Also the particles shape affects somewhat on Q_{ext} , but this is not considered in this study. If
6 the particles are assumed to be spherical, Q_{ext} can be calculated using a computer code based
7 on the Lorenz-Mie theory (Mishchenko et al., 2002). AOD is obtained by integrating σ_{ext}
8 over the total atmospheric column.

9 The differences between CS and σ_{ext} (at a certain height) as a function of particle size are
10 illustrated in Fig. 2. Both parameters are derived using the same aerosol size distribution (Fig.
11 2, left panel). The σ_{ext} is calculated using a refractive index of $m=1.48+0.003i$ and
12 wavelengths of 0.55 and 0.45 μm . As Fig. 2 shows, particles with D_p about 0.05-0.1 μm have
13 the largest contribution to CS, whereas for σ_{ext} the largest contribution is coming from
14 particles with D_p about 0.2-0.8 μm . The notable difference between the two quantities is that
15 particles $D_p < 0.1 \mu\text{m}$ can have a contribution to CS which is several orders of magnitude
16 larger than that to σ_{ext} . On the other hand, σ_{ext} is significantly more sensitive to particles with
17 $D_p > 1.0 \mu\text{m}$ than CS. It is clear that e.g. a large change in number concentration of the
18 smaller particle sizes would change the value of total CS when integrated over the size
19 distribution, but would have a minor effect on the value of σ_{ext} , and vice versa, if e.g. the
20 number concentration of large particles increased there would be little effect on CS. It is
21 noted that in addition to the theoretical differences the possibility of elevated aerosol layers
22 affect the column integrated values of σ_{ext} , i.e. the AOD, which must be considered when
23 comparing the satellite based AOD with in situ CS.

24 The response of σ_{ext} on changes in the particle size distribution depends to a certain extent on
25 the particle composition and the measurement wavelength. If the particle absorption is high
26 (i.e. the imaginary part of $m \sim 0.1i$), the contribution of particles $D_p < 0.1 \mu\text{m}$ to σ_{ext} would be
27 somewhat higher than in Fig. 2. Shorter wavelengths increase the sensitivity to smaller
28 particles, but as Fig. 2 illustrates, a 0.1 μm decrease in wavelength does not improve the
29 sensitivity significantly. Much shorter wavelengths would be needed to increase the
30 sensitivity of σ_{ext} to particles $D_p < 0.1 \mu\text{m}$, but such measurements could not be carried out in
31 a real atmosphere.

1

2 **4 Results**

3 The proxies as defined in Sect. 3 are formulated in terms of parameters which are either
4 obtained from ground-based in situ measurements (Eqs. 1-3) or from satellite data (Eqs. 4-7).
5 In this section the performance of these proxies is critically evaluated and in particular each
6 of the satellite-based parameters is critically examined.

7 **4.1 Comparison of condensation sink and aerosol optical depth**

8 Replacing CS with AOD is perhaps the most crucial assumption when determining the
9 proxies using satellite data, as indicated in Kulmala et al. (2011). Apart from the sensitivity
10 of these parameters for different particle sizes discussed in Section 3.1, other differences play
11 a role such as the vertical variation of the aerosol concentrations, the particle size range
12 considered and the dependence of aerosol particle size on relative humidity. CS is determined
13 from measured dry particle size distributions with a correction for ambient humidity. CS at
14 Botsalano and Marikana has been estimated from submicron size distribution while at
15 Elandsfontein size distributions up to 10 μm were used. In contrast, the AOD is an integrated
16 quantity with contributions from all optically active aerosols throughout the whole
17 atmospheric column. To assess the effect of these different factors on the relation between the
18 AOD and CS, the following comparisons are made:

- 19 1) In situ CS with nephelometer aerosol scattering coefficient
- 20 2) In situ nephelometer aerosol scattering coefficient with AOD from AERONET
- 21 3) In situ CS with AOD from both AERONET- and satellite measurements.

22 Coincident measurements of size distributions to derive the CS and aerosol scattering
23 coefficients from a nephelometer are only available from the Elandsfontein measurement
24 station. The comparison between CS and scattering coefficient serves to eliminate effects of
25 the vertical variation of the aerosol concentrations on the comparison. The nephelometer
26 measures the dry particle scattering at 0.525 μm wavelength and the results are presented at
27 Standard Temperature and Pressure (STP) atmosphere. The maximum particle size is limited
28 to $D_p \sim 10 \mu\text{m}$. It is noted that the nephelometer considers only aerosol scattering, and not the
29 total extinction which would also require information on absorption. However, the
30 contribution of absorption to the total aerosol extinction is generally much smaller than
31 scattering. Laakso et al. (2012) reported that at Elandsfontein the absorption was increased
32 during the coldest months (May-Oct.) due to biomass burning, domestic burning of coal for

1 heating and cooking, contributing about 15-20% to the total aerosol extinction whereas
2 during the warmer months (Nov.-Apr.) absorption contributed ~10% of the total aerosol
3 extinction. To take the seasonal variation of absorption into account, the CS and the
4 scattering coefficients were compared separately for the periods May-Oct. and Nov.-Apr.
5 The results in Fig. 3 show that for both periods scattering coefficients and CS were well-
6 correlated with $R^2=0.67$ for Nov.-Apr., and $R^2=0.71$ for May-Oct. The R^2 values were higher
7 than those from measurements at a clean continental boreal forest measurement site in
8 Hyytiälä, Southern Finland ($R^2=0.38$, Virkkula et al., 2011).

9 The next step is to compare the nephelometer scattering coefficient to the AOD to evaluate
10 effects of the possible occurrence of elevated aerosol layers and/or boundary layer mixing.
11 Also the presence of large dust particles might have some effect on the comparison due to the
12 limited particle size in the nephelometer inlet. In this comparison we first compare with
13 AERONET measurements of AOD at Elandsfontein, which are more accurate than those
14 retrieved from satellite data. As Fig. 4 shows, the correlations between the AERONET AOD
15 and the in situ scattering coefficient (warm season $R^2=0.46$, cold season $R^2=0.24$) are lower
16 than those between the CS and the scattering coefficient. This indicates that the elevated
17 aerosol layers and boundary layer mixing might affect more than the theoretical differences
18 when estimating the sink of pre-existing aerosols by using the AOD.

19 For the comparison of CS with the AOD retrieved from MODIS, daily AOD values were
20 used which are spatial averages of the observations within 3 km radius from each
21 measurement station. As Fig. 5 shows, the CS- vs. satellite AOD data are scattered all over
22 the graph and although there is a tendency of increasing CS with increasing AOD there is no
23 apparent correlation ($0.03 \leq R^2 \leq 0.06$). As an alternative, a bivariate method (York et al.,
24 2004) was applied to account for the uncertainties associated to both CSs and MODIS AODs
25 in the fitting. For CS the uncertainty was assumed to be 10% (Petäjä et al., 2013) and for
26 MODIS AOD an uncertainty of 0.05+15% was used (Levy et al., 2013). This means that for
27 low AOD the relative uncertainty is rather high, e.g. for AOD=0.1 the relative uncertainty
28 would be 65%. As Fig. 5 shows the bivariate method gave very different results than LSQ.

29 At Marikana and Elandsfontein the largest observed AODs are not related to largest CS,
30 which could be due to the presence of elevated aerosol layers. In a recent study by
31 Giannakaki et al., (2015) data from a ground-based lidar at Elandsfontein are analyzed and
32 the results show that the mean contribution of elevated aerosol layers to the AOD is 46%.
33 To estimate the effect of elevated aerosol layers on the CS-AOD comparison at Marikana,

1 CALIPSO observations of aerosol vertical extinction profiles are used. All CALIPSO
2 daytime overpasses between 8.2.2008 and 17.5.2010 within 50 km from the Marikana station
3 were considered. Due to the small CALIPSO swath width only 48 days of data are available.
4 At Marikana the median MODIS AOD is 0.15 for the whole measurement period, and as Fig.
5 5 shows, the CS values are less scattered when AODs are smaller than the median. Therefore
6 the vertical aerosol extinction profiles from CALIPSO are studied separately for the cases
7 where MODIS AOD ≤ 0.15 and AOD > 0.15 . As Fig. 6 shows, for higher AODs the median
8 extinction profile indicates an elevated aerosol layer, which supports the result that high
9 AODs also at Marikana are likely to be associated with an elevated aerosol layer.

10

11 **4.2 Proxies defined from the in situ data and comparison with N_{nuc}**

12 The proxies are first computed using in situ measurements from Marikana and Elandsfontein
13 following Eqs. 1-3 to evaluate how well each of them could predict the nucleation mode
14 number concentration within our study area. It is noted that due to different instrumentation
15 N_{nuc} from Marikana consists of particles with $D_p < 30$ nm, but at Elandsfontein N_{nuc} consists
16 of particles with D_p 10-30 nm. In addition, CS at Marikana is defined from submicron
17 particles whereas at Elandfontein CS is defined from particles with $D_p < 10 \mu m$.

18 Figure 7 shows the diurnal variation of each of the in situ proxy components and the number
19 concentration of nucleation mode particles. At Marikana the N_{nuc} median peaks about 10 a.m.,
20 and at Elandsfontein about an hour later. At the time of the satellite overpass the median of
21 N_{nuc} is lower than before noon at both locations, and about the same order of magnitude. The
22 diurnal variation of NO_x -NO and SO_2 concentrations show somewhat different characteristics
23 at Marikana than at Elandsfontein, The morning and evening peaks of NO_x -NO at Marikana
24 are most likely associated with household combustion and traffic whereas the single SO_2
25 peak in the morning is most likely related to the industrial emissions and the break-up of the
26 inversion layers that form quite regularly in the South African Highveld (Venter et al., 2012).
27 At Elandsfontein, where the major emission source is heavy industry, an increase in the NO_x -
28 NO and the SO_2 concentration medians are seen about 10 a.m. The median of SO_2
29 concentration decreases in the late afternoon while the median of NO_x -NO concentration does
30 not vary much. At the time of the satellite overpass the NO_x -NO and SO_2 medians are much
31 higher at Elandsfontein than at Marikana. Results show also that at the time of the satellite
32 overpass NO_x -NO and SO_2 are positively correlated; at Elandsfontein $R^2=0.58$, and at

1 Marikana $R^2=0.32$ are obtained. At Elandsfontein CS does not show any clear diurnal
2 variation and it is systematically lower than at Marikana. Also at Marikana the diurnal
3 variation of the CS is rather weak during the daytime but a peak in the median is seen in the
4 evening.

5 Figure 8 shows the diurnal variation of the in situ proxies at Marikana and Elandsfontein. The
6 comparison of the diurnal variation of the proxies and N_{nuc} indicates that the proxy- N_{nuc}
7 relation depends on the time of the day. At the time of the satellite overpass (13-14 LT) the
8 highest correlation with N_{nuc} at Marikana is obtained with the SO_2/CS -proxy ($R^2=0.22$, Fig.9),
9 but at Elandsfontein the correlation remains below 0.1. At Marikana the correlation of N_{nuc}
10 with $SO_2 \cdot UV/CS^2$ - proxy (Eq. 1) is less good at the time of the satellite overpass but at 9-10
11 a.m. $R^2 = 0.25$. On the other hand the $(NO_x-NO)/CS$ and UV/CS^2 proxies do not perform well
12 in predicting N_{nuc} . Also, it is noted that at the time of the satellite overpass all the proxy
13 values show much higher median values at Elandsfontein than at Marikana while the median
14 for N_{nuc} is about the same at both locations. At Elandsfontein somewhat better correlations
15 with N_{nuc} are observed if only the source terms of the proxies are considered. For example,
16 the values of R^2 between N_{nuc} and $SO \cdot UV$ are 0.35 at 10-11 LT, and 0.14 at 13-14 LT,
17 respectively, but when the sink-term CS^2 is included in the proxy there is no correlation. At
18 Marikana CS doesn't have as high influence on the proxy performance as at Elandsfontein.

19 The difference with the results reported for Southern Finland (Kulmala et al. (2011)) is that in
20 our study SO_2 has a strong effect on the performance of the proxy: without SO_2 the UV/CS^2 –
21 term does not correlate with N_{nuc} . Given that the satellite data are associated much higher
22 uncertainties than the in situ measurements, these in situ-based results can be considered as
23 some kind of upper limits for the overall performance of the proxies computed using satellite
24 data (Eqs. 4-7).

25 .

26 **4.3 Proxies using satellite data**

27 **4.3.1 Spatial pattern of the satellite-based proxies**

28 Each of the satellite based parameter is analyzed from Jan. 2007 to Dec. 2010. Figure 11
29 shows the four year medians of SO_2 and NO_2 column densities obtained from the OMI
30 instrument, as well as the AOD at 550 nm from MODIS Aqua observations. Daily satellite
31 data is used to define the satellite-based proxies over the study area (Eq. 4-7). Figure 12
32 shows the four year median spatial patterns for the four satellite-based proxies. The spatial

1 patterns of these four proxies are quite different and in particular there is large difference
2 between the spatial variation of the regional proxies and that of the proxies for nucleation
3 from primary emissions. As expected, the latter strongly reflect the spatial distributions of the
4 precursor gases with high concentration over the Highveld industrial area, where the values
5 of NO₂ and SO₂ columns are high and the sink (AOD) is low. For the NO₂/AOD proxy also
6 elevated values are observed over the Johannesburg-Pretoria area while for the other proxies
7 a local minimum occurs over these cities.

8 All the four satellite proxies show larger values at Elandsfontein than at Marikana, which is
9 consistent with the results obtained for the in situ proxies. Based on the in situ results the
10 SO₂-related proxies are expected to predict N_{nuc} at the time of the satellite overpass better
11 than the other proxies. Comparison of the spatial patterns of each proxy calculated using
12 satellite data in the vicinity of the in situ measurement stations shows that there are not very
13 much difference between the spatial pattern of SO₂- and NO₂-related proxies.

14 The propagation of relative uncertainty associated with the proxies using satellite data can be
15 estimated by comparing the uncertainties related to each satellite parameter (Sect. 3) and the
16 observed median values shown in Fig. 11. For example, over background areas where both
17 AOD and SO₂ are low, the SO₂ ·UV-B /AOD² -proxy can have an uncertainty of over 90%.
18 On the other hand, over source areas where both NO₂ and AOD are slightly elevated the
19 NO₂/AOD proxy would have an uncertainty of about 50%. Generally over South Africa the
20 uncertainty in satellite-based proxies is high, especially over areas where both low values of
21 NO₂, SO₂ and AOD are frequently observed.

22

23 **4.3.2 Comparison of satellite and in situ proxy components**

24 Before evaluating the performance of the proxies using satellite data, first the quality of the
25 parameters used in these proxies should be examined. The CS/AOD comparison was
26 discussed in Sect. 4.1. Here we compare satellite data for NO₂, SO₂ and UV-B with in situ
27 data at each of the measurement stations. The satellite data for each station is collected
28 within a 12 km (NO₂, SO₂, UV-B) or a 3 km (AOD) radius from the station and the results
29 are compared with hourly means of the in situ data extracted between 13-14 LT, i.e. ± 30 min
30 within the approximate satellite overpass.

31 The satellite NO₂ column densities and the in situ NO_x-NO concentrations are reasonably
32 well correlated as are the satellite UV-B irradiances and the global radiation measured at each

1 station. The highest correlation for NO₂ were obtained at Marikana ($R^2=0.55$), and lowest at
2 Elandsfontein ($R^2=0.26$). For UV-B and global radiation the correlations were $0.61 \leq R^2$
3 ≤ 0.77 . In Kulmala et al. (2011) a constant value was assumed for the satellite-based SO₂
4 when defining the global proxy maps, because the SO₂ product they used (middle
5 tropospheric SO₂) did not show reasonable spatial pattern. In this study the middle -
6 troposphere SO₂ data was replaced by the OMI boundary layer product (Sec. 3), which
7 improved the characterization of the SO₂ spatial variation (Fig. 10). However, the relative
8 uncertainty in the satellite-based SO₂ remains still high, unless the data is averaged over a
9 long time period/ large spatial area. At all three stations lower correlation between the
10 satellite and in situ based SO₂ measurements were obtained than for the other source
11 parameters, at Marikana there is practically no correlation. Similar results were obtained
12 when the satellite- and in situ-based proxies were compared (Table 2, figures in the
13 supplementary material). Overall large differences exist between the satellite proxies and in
14 situ proxies.

15 Since at Marikana and Elandsfontein the in situ data showed correlation between the (NO_x-
16 NO) and the SO₂ concentrations, the satellite NO₂ column density is also compared with the
17 in situ SO₂. Results show that in fact the OMI NO₂ compares better with the in situ SO₂ than
18 the actual OMI SO₂ product. At Elandsfontein $R^2=0.25$, and at Marikana $R^2=0.31$ are
19 obtained between the satellite NO₂ column and in situ SO₂ concentration.

20

21 **4.3.3 Comparison of satellite-based proxies with N_{nuc}**

22 To further evaluate the performance of the satellite-based proxies, they are compared with the
23 in situ N_{nuc}. Only data from Elandsfontein and Marikana are included in the comparinson
24 since the number of coincident N_{nuc} and satellite proxy observations was too low at the other
25 stations. As expected, neither of the two satellite-based SO₂ – proxies are able to predict N_{nuc}.
26 Interestingly, the only case where weak correlation is obtained between a proxy using
27 satellite data and N_{nuc} is for the NO₂/AOD (Fig 12). This result is very different than what is
28 expected based on the comparison of the in situ proxies and N_{nuc}. In fact, the connection
29 between NO₂/AOD and N_{nuc} is most probably related to the correlation between the satellite
30 NO₂ column density and the in situ SO₂ concentration. If the source term in the SO₂·UV-
31 B/AOD² proxy was replaced by NO₂·UV-B, the correlation with N_{nuc} at Elandsfontein would
32 be $R^2=0.23$, and at Marikana $R^2=0.06$. This implies that over areas where SO₂ and NO₂ are

1 affected by some common factors, e.g. emission sources, the satellite NO₂ could be a better
2 estimate for the source term than SO₂.

3

4 **5 Conclusions**

5 This work explores the use of proxies using satellite data to obtain information on the
6 concentration of nucleation mode aerosol particles (N_{nuc}). These proxies have been
7 formulated using relations derived from data on ground-based nucleation and precursor gases,
8 which were simplified for the use of satellite data in Kulmala et al. (2011). The
9 simplifications and associated assumptions are critically examined. In this study data were used
10 over part of South Africa where ground-based observations are available from four
11 experimental sites, for comparison with both the satellite-based parameters used in the proxy
12 formulations and for comparison of the proxies with ground-based measurements of the
13 nucleation mode aerosol particle number concentrations. For the computation of the proxies,
14 data from the A-train satellites are used. The NO₂, SO₂ and UV-B radiation are obtained from
15 the OMI instrument and AOD from the MODIS instrument. The NO₂ and UV-B data are the
16 same than what was used in Kulmala et al. (2011), but the AOD was upgraded to the newest
17 collection 6 3 km product. Also the SO₂ product was changed to the planetary boundary layer
18 product (OMI SO₂ PBL) that represents the total column values with a priori assumption that
19 the emissions are mainly in the boundary layer. The satellite observations are also extensively
20 compared with in situ data.

21 Based on the proxies derived from the in situ data it is expected that the SO₂-related proxies
22 would be the best predictors of N_{nuc} within the study area at the time of the satellite overpass
23 (13-14 LT). It is also noted that even though the in situ NO₂/CS proxy did not do well in
24 predicting N_{nuc} , a positive correlation between the SO₂ and NO₂ concentrations is found at the
25 measurement stations (at 13-14 LT). The R^2 between in situ SO₂/CS and N_{nuc} is 0.22 and this
26 value could be considered as some kind of “upper limit” for the satellite proxies, for which
27 uncertainties are much higher than for the in situ proxies. Using ground-based data, Kulmala
28 et al. (2011) reported that SO₂ had only moderate influence on the performance of the
29 SO₂ ·UV/CS² proxy in Southern Finland. The overall correlation between this proxy and N_{nuc}
30 over South Africa was even lower ($R^2=0.13$) than over Southern Finland ($R^2=0.29$), yet our
31 results clearly indicate a strong influence of SO₂ on the performance of the proxy. If the SO₂
32 was excluded from the proxy, no correlation with in situ proxies and N_{nuc} was found.

1 Kulmala et al., (2011) emphasized that the most crucial assumption in deriving the satellite
2 based proxies was the replacement of the CS with AOD. This assumption is further evaluated
3 in the current study using several tests. A fundamental reason for differences between CS and
4 AOD is the intrinsic dependence on different aerosol size ranges, with CS more sensitive to
5 very small particles (smaller than about 200 nm) and AOD more sensitive to particles larger
6 than that. Yet, good correlation is obtained between measured scattering coefficients for dry
7 aerosol and CS evaluated from collocated particle size distribution measurements. When the
8 in situ scattering coefficients or CS are compared with collocated AOD measurements the
9 correlation decreases. This may be due to several effects. In particular the presence of
10 elevated aerosol layers and/or large dust particle increases the AOD but does not affect the
11 CS. However, overall the AOD is rather low (<0.1) over the major part of the study area,
12 which means that these values are also associated with substantial relative uncertainty, which
13 needs to be accounted for when deriving the satellite-based proxies.

14 Even though the OMI SO₂ PBL data product showed a distinct improvement in describing the
15 spatial patterns of SO₂ as compared to the dataset used in Kulmala et al. (2011), the satellite-
16 based SO₂ did not describe well the day-to-day variations at the measurement stations. In
17 addition, the observed SO₂ column values were often close to the noise level associated with
18 a single column retrieval reported by Krotkov et al. (2008). The only relation between a
19 satellite-based proxy and N_{nuc} was obtained for NO₂/AOD (at Elandsfontein R²=0.24, and at
20 Marikana R²=0.09). The result is different than what was expected based on the in situ
21 proxies. The most probable explanation is the positive correlation between the ground-based
22 NO₂ and SO₂ concentrations within the study area. It is found that in fact the satellite NO₂
23 column correlates better with in situ SO₂ concentration than the satellite SO₂ column, where
24 no correlation was found.

25 Overall this study shows that the uncertainties related to the satellite products remain a major
26 issue in this satellite-based proxy approach, especially over areas like South Africa, where the
27 AOD and the SO₂, and NO₂ concentrations are generally relatively low. Throughout the
28 whole study the relative uncertainties related to the satellite-based proxies were well above
29 50%. In For the NO₂/AOD proxy the largest relative uncertainties were often related to AOD.
30 Otherwise SO₂ was clearly the most uncertain component in the proxies calculated using
31 satellite data. Despite these uncertainties related to the satellite data, the in situ data did not
32 do significantly better in predicting N_{nuc} within our study area. This indicates that overall
33 improvements in the formulation of the proxies are needed.

1

2 **Acknowledgements**

3 This work is supported by Academy of Finland (1251427, 1139656, Finnish Centre of
4 Excellence in Atmospheric Science 272041), European Research Council (ATMNUCLE),
5 The European Integrated project on Aerosol Cloud Climate and Air Quality Interactions
6 (EUCAARI), and the ESA projects Aerosol-cci (ESA-ESRIN project AO/1-6207/09/I-LG
7 and ALANIS-Aerosols (Contract no. 4200023053/10/I-LG, STSE-ALANIS Atmosphere-
8 Land Interactions Study Theme 3: Aerosols). Eskom and Sasol supplied logistical support for
9 measurements at Elandsfontein, while the town council of Rustenburg supplied support to the
10 measurement at Marikana. The OMI NO₂, SO₂ and UV data were obtained from the NASA
11 Mirador service maintained by Goddard Earth Sciences Data and Information Services
12 Center (GES DISC). The OMI surface UV data were obtained from the NASA Aura
13 Validation Data Center (AVDC). The MODIS Aqua data were provided by NASA LAADS
14 Web, and the CALIPSO data was obtained from NASA Atmospheric Science Data Center
15 (ASDC).

1 **References**

- 2 Beukes, P., Vakkari, V., van Zyl, P. G., Venter, A., Josipovic, M., Jaars, K., Tiitta, P.,
3 Kulmala, M., Worsnop, D., Pienaar, J., Virkkula, A., and Laakso L.: Source region plume
4 characterisation of the interior of South Africa, as measured at Welgegund, *Clean Air Journal*,
5 Vol. 23, No. 1, 2013.
- 6 Bucselá, E. J., Krotkov N., Celarier, E., Lamsal, L., Swartz, W., Bhartia, P., Boersma, K.,
7 Veefkind, J.P., Gleason, J., and Pickering, K.: A new stratospheric and tropospheric NO₂
8 retrieval algorithm for nadir-viewing satellite instruments: applications to OMI. *Atmos. Meas.*
9 *Tech*, 6, 2607-2626, doi: 10.5194/amt-6- 2607-2013, 2013.
- 10 Burrows, J.P., U. Platt and P.Borrell (Editors) *The Remote Sensing of Tropospheric*
11 *Composition from Space*, 536 pp., Springer-Verlag Berlin Heidelberg 2011. ISBN: 978-3-
12 642-14790-6 doi: 10.1007/978-3-642-14791-3., pp. 359-313.
- 13 Crippa, P., Spracklen, D., and Pryor, S.C.: Satellite-derived estimates of ultrafine particle
14 concentrations over Eastern North America. *J. Geophys. Res.*, 118, 9968-9981, 2013.
- 15 Dal Maso, M., Kulmala, M., Riipinen, I., Wagner, R., Hussein, T., Aalto, P. P. & Lehtinen, K.
16 E. J.: Formation and growth of fresh atmospheric aerosols: eight years of aerosol size
17 distribution data from SMEAR II, Hyytiälä, Finland. *Boreal Env. Res.* 10, 323–336, 2005.
- 18 Fioletov, V.E., McLinden, C.A., Krotkov, N., Moran, M.D., and Yang, K.; Estimation of SO₂
19 emissions using OMI retrievals. *Geophys. Res. Lett.*, vol. 38, L21811,
20 doi:10.1029/2011GL049402, 2011.
- 21 Giannakaki, E., Pfüller, A., Korhonen, K., Mielonen, T., Laakso, L., Vakkari, V., Baars, H.,
22 Engelmann, R., Beukes, J. P., Van Zyl, P. G., Josipovic, M., Tiitta, P., Chiloane, K., Piketh,
23 S., Lihavainen, H., Lehtinen, K. E. J., and Komppula, M.: One year of Raman lidar
24 observations of free tropospheric aerosol layers over South Africa. *Atmos. Chem. Phys.*
25 *Discuss.*, 15, 1343-1384, doi:10.5194/acpd-15-1343-2015, 2015.
- 26 Hirsikko, A., Vakkari, V., Tiitta, P., Manninen, H.E., Gagné, S., Laakso, H., Kulmala, M.,
27 Mirme, A., Mirme, S., Mabaso, D., Beukes, J.P., and Laakso, L.: Characterisation of sub-
28 micron particle number concentrations and formation events in the western Bushveld Igneous
29 Complex, South Africa. *Atmos. Chem. Phys*, 12, 3951-3967, 2012.
- 30 Hirsikko, A., Vakkari, V., Tiitta, P., Hatakka, J., Kerminen, V.-M., Sundström, A.-M.,
31 Beukes, J.P., Manninen, H.E., Kulmala M., and Laakso, L.: Multiple daytime nucleation

1 events in semi-clean savannah and industrial environments in South Africa: analysis based on
2 observations. *Atmos. Chem. Phys.*, 13, 5523-5532, 2013.

3 Holben, B., Eck, T.F., Slutsker, I., Tanre, D., Buis, J.P., Setzer, A., Vermote, E., Reagan, J.
4 A., Kaufman, Y. J. , Nakajima, T. , Lavenu, F. , Jankowiak, I. and Smirnov, A.: AERONET
5 - A Federated Instrument Network and Data Archive for Aerosol Characterization. *Rem. Sens.*
6 *Environ.*, vol. 66, 1-16, 1998.

7 IPCC, Intergovernmental Panel on Climate Change, Fifth Assessment Report: Climate
8 Change. Cambridge University Press, Cambridge, United Kingdom and New York, NY, USA,
9 2013.

10 Kokhanovsky, A.A., and de Leeuw Gerrit (editors): *Satellite Aerosol Remote Sensing over*
11 *Land*, Springer, Berlin, Germany, 2009.

12 Krotkov, N., Carn, S., Krueger A., Bhartia, P., and Yang, K.: Band residual difference
13 algorithm for retrieval of SO₂ from the Aura Ozone Monitoring Instrument (OMI). *IEET T.*
14 *Geosci. Remote*, 44, 12591266, 2006.

15 Krotkov, N., McClure, B., Dickerson, R., Carn, S., Li, C., Bhartia, P., Yang, K., Krueger, A.,
16 Li, Z., Levelt, P., Chen, H., Wang, P., and Lu, D.: Validation of SO₂ retrievals from the
17 Ozone Monitoring Instrument over NE China. *Journal of Geophys. Res.*, Vol. 113, D16S40,
18 doi:10.1029/2007JD008818, 2008.

19 Kulmala, M., Vehkamäki, H., Petäjä, T., Dal Maso, M., Lauri, A., Kerminen, V.-M., Birmili,
20 W., and McMurry, P.H.: Formation and growth rates of ultrafine atmospheric particles: a
21 review of observations. *J. Aerosol Sci.*, 35, 143-176, 2004.

22 Kulmala, M., Petäjä, T., Mönkkönen, P., Koponen, I.K., Dal Maso, M., Aalto, P.P., Lehtinen,
23 K.E.J., and Kerminen, V.-M.: On the growth of nucleation mode particles: source rates of
24 condensable vapor in polluted and clean environments. *Atmos. Chem. Phys.* 5, 409-416, 2005.

25 Kulmala, M., and Kerminen, V.-M.: On the formation and growth of atmospheric
26 nanoparticles. *Atm. Res.*, 90, 132-150, 2008.

27 Kulmala, M., Arola, A., Riuttanen, L., Sogacheva, L., de Leeuw, G., Kerminen, V.-M. and
28 Lehtinen, K.E.J.: The first estimates of global nucleation mode aerosol concentrations based
29 on satellite measurements. *Atmos. Chem. Phys.* 11, 10791-10801, 2011.

30 Laakso, L., Laakso, H., Aalto, P.P, Keronen, P., Nieminen, T., Pohja, T., Siivola, E., Kulmala,
31 M., Kgabi, N., Molefe, M., Mabaso, D., Phalatse, D., Piennaar, K., and Kerminen, V.-M.:

1 Basic characteristics of atmospheric particles, trace gases and meteorology in a relatively
2 clean Southern African Savannah environment, *Atmos. Chem. Phys.*, 8, 4823-4839, 2008.

3 Laakso, L., Vakkari, V., Virkkula, A., Laakso, H., Backman, J., Kulmala, M., Beukes, J.P.,
4 van Zyl, P.G., Tiitta, P., Josipovic, M., Pienaar, J.J., Chiloane, K., Gilardoni, S., Vignati, E.,
5 Wiedensohler, A., Tuch, T., Birmili, W., Piketh, S., Collett, K., Fourie, G.D., Komppula, M.,
6 Lihavainen, H., de Leeuw, G., and Kerminen, V.-M.: South African EUCAARI
7 measurements: seasonal variation of trace gases and aerosol optical properties. *Atmos. Chem.*
8 *Phys.*, 12, 1847-1864, 2012.

9 Lamsal, L. N., Krotkov, N. A., Celarier, E. A., Swartz, W.H., Pickering, K. E., Bucsele, E. J. ,
10 Gleason, J. F., Martin, R.V., Philip, S., Irie, H., Cede, A., Herman, J., Weinheimer, A.,
11 Szykman, J.J., Knepp, T. N.: Evaluation of OMI operational standard NO₂ column retrievals
12 using in situ and surface-based NO₂ observations. *Atmos. Chem. Phys.*,14, 11587–11609,
13 doi:10.5194/acp-14-11587-2014, 2014.

14 Lee, K. H., Li, Z., Kim, Y. J., & Kokhanovsky, A.: Atmospheric aerosol monitoring from
15 satellite observations: a history of three decades. In *Atmospheric and biological*
16 *environmental monitoring*, Springer Netherlands, 2009.

17 Lehtinen, K. E. J., Korhonen, H., Dal Maso, M., and Kulmala, M.: On the concept of
18 condensation sink diameter. *Boreal Env. Res.*, 8, 405-411, 2003.

19 Levy, R.C., Mattoo, S., Munchak, L.A., Remer, L.A., Sayer, A.M., Patadia, F., and Hsu
20 N.C. : The Collection 6 MODIS aerosol products over land and ocean. *Atmos. Meas. Tech.*,
21 6, 2989-3034, 2013.

22 Lourens, A. S. M., Beukes, J. P., Van Zyl, P. G., Fourie, G. D., Burger, J. W. , Pienaar, J. J.,
23 Read, C. E., and Jordaan, J. H.: Spatial and Temporal assessment of gaseous pollutants in the
24 Highveld of South Africa, *S. Afr. J. Sci.*, 107, No. 269, 8 pp., doi:10.4102/sajs.v107i1/2.269,
25 2011.

26 Lourens, A. S. M., Butler, T. M., Beukes, J. P., Van Zyl, P. G., Beirle, S., Wagner, T., Heue,
27 K-P., Pienaar, J. J., Fourie, G. D., Lawrence, M.G.: Re-evaluating the NO₂ hotspot over the
28 South African Highveld, *S. Afr. J. Sci.*, 108(9/10), Art. #1146, 6 pages. DOI: 10.4102/sajs.
29 v108i11/12.1146, 2012.

30 Maritz, P., Beukes, J. P., Van Zyl, P. G., Conradie, E.H., Liousse, C., Galy-Lacaux, C.,
31 Castéra, P., Ramandh, A., Mkhathshwa, G., Venter, A.D. and Pienaar, J.J.: Spatial and

1 temporal assessment of organic and black carbon at IDAF sites in South Africa, submitted to
2 Environ. Mon. Assess., 2014.

3 Mielonen, T., Levy, R.C., Aaltonen, V., Komppula, M., de Leeuw, G., Huttunen, J.,
4 Lihavainen, H., Kolmonen, P., Lehtinen, K.E.J., and Arola, A.: Evaluating the assumptions of
5 surface reflectance and aerosol type selection within the MODIS aerosol retrieval over land:
6 the problem of dust type selection. *Atmos. Meas. Tech.*, 4, 201–214, 2011.

7 Mishchenko, M. I., L. D. Travis, and A. A. Lacis: *Scattering, Absorption, and Emission of*
8 *Light by Small Particles*. Cambridge University Press, Cambridge, 2002.

9 Petäjä, T., Maudin III, R.L., Kosciuch, E., McGrath, J., Nieminen, T., Paasonen, P., Boy, M.,
10 Adamov, A., Kotiaho, T., and Kulmala, M.: Sulfuric acid and OH concentrations in a boreal
11 forest site. *Atmos. Chem. Phys.*, 9, 7435-7448, 2009.

12 Petäjä, T., Vakkari, V., Pohja, T., Nieminen, T., Laakso, H., Aalto, P.P., Keronen, P., Siivola,
13 E., Kerminen, V.-M., Kulmala, M., and Laakso, L.: Transportable Aerosol Characterization
14 Trailer with Trace Gas Chemistry: Design, Instruments and Verification. *Aerosol Air Qual.*
15 *Res.*, 13: 421–435, 2013.

16 Schnelle-Kreis, J., Küpper, U., Sklorz, M., Cyrys, J., Briedé, J. J., Peters, A., and Zimmerman,
17 R.: Daily measurements of organic compounds in ambient particulate matter in Augsburg,
18 Germany: new aspects on aerosol sources and aerosol related health effects. *Biomarkers*, 14
19 (SI), 39-44, 2009.

20 Seaton, A., MacNee, W., Donaldson, K., Godden, D.: Particulate air pollution and acute
21 health effects. *The Lancet*, 345, 176-178, 1995.

22 Shi, Y., Zhang, J., Reid, J.S., Hyer, E.J., and Hsu, N.C.: Critical evaluation of the MODIS
23 Deep Blue aerosol optical depth product for data assimilation over North Africa. *Atmos.*
24 *Meas. Tech.*, 6, 949-969, 2013.

25 Tanskanen, A., Krotkov, N.A., J.R. Herman, and Arola, A.: Surface Ultraviolet Irradiance
26 From OMI. *IEEE Trans. Geosci. Remote Sens.*, Vol. 44, No. 5, 1267-1271, 2006.

27 Utell, M.J., and Frampton, M.W.: Acute Health Effects of Ambient Air Pollution: The
28 Ultrafine Particle Hypothesis. *J Aerosol Med Pulm Drug Deliv.*, Vol. 13, 4, 355-359, 2000.

29 Vakkari, V., Laakso, H., Kulmala, M., Laaksonen, A., Mabaso, D., Molefe M., Kgabi, N.,
30 and Laakso, L.: New particle formation events in semi-clean South African savannah. *Atmos.*
31 *Chem. Phys.*, 11, 3333-3346, 2011.

1 Vakkari, V., Beukes, J.P., Laakso, H., Mabaso, D., Pienaar, J.J., Kulmala, M., and Laakso,
2 L.: Long-term observations of aerosol size distributions in semi-clean and polluted savannah
3 in South Africa. *Atmos. Chem. Phys.*, 13, 1751–1770, 2013.

4 Veefkind, J.P., Boersma, K.F., Wang, J., Kurosu, T.P., Krotkov, N., Chance, K., and Levelt,
5 P.F.: Global satellite analysis of the relation between aerosols and short-lived trace gases.
6 *Atmos. Chem. Phys.*, 11, 1255-1267, 2011.

7 Venter, A.D., Vakkari, V., Beukes, J.P., van Zyl, P.G., Laakso, H., Mabaso, D., Tiitta, P.,
8 Josipovic, M., Kulmala, M., Pienaar, J.J., and Laakso, L.: An air quality assessment in the
9 industrialised western Bushveld Igneous Complex, South Africa. *S. Afr. J. Sci.*, 108(9/10), No.
10 1059, doi:10.4102/sajs.v108i9/10.1059, 2012.

11 Virkkula, A., Backman, J., Aalto, P.P., Hulkkonen, M., Riuttanen, L., Nieminen, T., dal Maso,
12 M., Sogacheva, L., de Leeuw, G., and Kulmala, M.: Seasonal cycle, size dependencies, and
13 source analyses of aerosol optical properties at the SMEAR II measurement station in
14 Hyytiälä, Finland. *Atmos. Chem. Phys.*, 11, 4445-4468, 2011.

15 Winker, D. M., Hunt, W. M., and McGill, M.J.: Initial performance assessment of CALIOP.
16 *Geophys. Res. Lett.*, Vol. 34, L19803, doi:10.1029/2007GL030135, 2007.

17 York, D., Evensen, N., Martinez, M., and Delgado, J.: Unified equations for the slope,
18 intercept, and standard errors of the best straight line. *Am. J. Phys.*, 72(3), 367–375, 2004.

19

1

2 Table 1. A summary of the measurements used in this study. Here are listed only
 3 measurements between the study period 1.1.2007-31.12.2010.

Instrument	Measurement area/ Location	Measurement period	Measured parameters
Ozone Monitoring instrument OMI (satellite)	25.0-28.0S, 25.5-30.5E (whole study area)	Jan. 2007-Dec. 2010, obs. appr. once/day, only cloud-free obs.	NO ₂ and SO ₂ column densities, UV-B irradiance
Moderate Imaging Spectroradiometer MODIS (Aqua, satellite)	25.0-28.0S, 25.5-30.5E (whole study area)	Jan. 2007-Dec. 2010, obs. appr. once/day, only cloud-free obs.	Column integrated aerosol optical depth AOD at 550 nm wavelength
Cloud-Aerosol Lidar with Orthogonal Polarization CALIOP (satellite based lidar)	Selected locations within the study area	Selected days between Jan. 2007-Dec. 2010	Vertical profile of aerosol extinction at 532 nm wavelength
Aerosol Robotic Network AERONET Sunphotometer (in situ)	Elandsfontein (26.25S, 29.42E)	Mar. – Dec. 2010, only cloudfree obs. during daylight.	Column integrated aerosol optical depth AOD at 500 nm wavelength.
Nephelometer (in situ)	Elandsfontein	Mar. – Dec. 2010	Aerosol scattering coefficient
Differential Mobility Particle Sizer DMPS (in situ)	Marikana (25.70S,27.48E) Botsalano (25.54S, 25.75E) Welgegund (26.57S, 26.94E)	Marikana: Feb 2008-May 2010 Botsalano: Jan. 2007-Feb. 2008 Welgegund: May-Dec. 2010	Particle size distribution, condensation sink, event classification
Scanning Mobility Particle Sizer SMPS (in situ)	Elandsfontein All in situ stations	Mar. – Dec. 2010 dates/station as above	Particle size distribution, condensation sink NO _x , and NO, SO ₂ , global radiation, T, RH

1 Table 2. Correlations between in situ- and satellite-based proxies. The number of coincident
 2 observations is denoted with “N”. Scatter plots for each of the case are provided as a
 3 supplementary material.

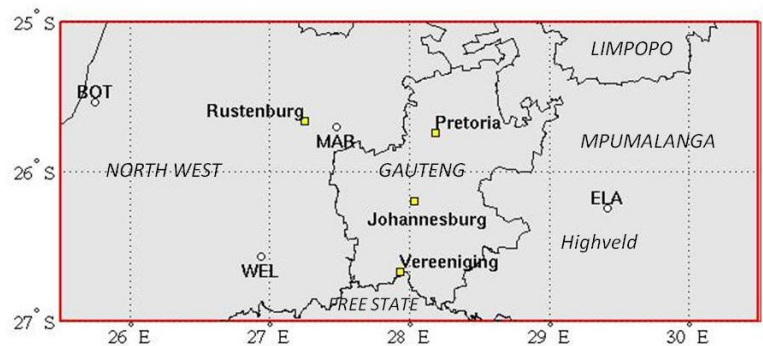
Station	(NO _x -NO)/CS vs. NO ₂ /AOD	SO ₂ /CS vs. SO ₂ /AOD	SO ₂ ·UV-B/cs ² vs. SO ₂ ·UV-B/AOD ²	Glob./CS ² vs UV-B/AOD ²
Elandsfontein	R ² = 0.11, N=46	R ² = 0.20, N=41	R ² =0.13, N=39	R ² = 0.30, N=52
Marikana	R ² = 0.38, N=93	R ² = 0.005, N=76	R ² =0.13, N=76	R ² =0.22, N=117
Botsalano	R ² =0.004, N=16	R ² = 0.12, N=14	R ² =0.30, N=14	R ² =0.11, N=18

4

5

1 Figures

2

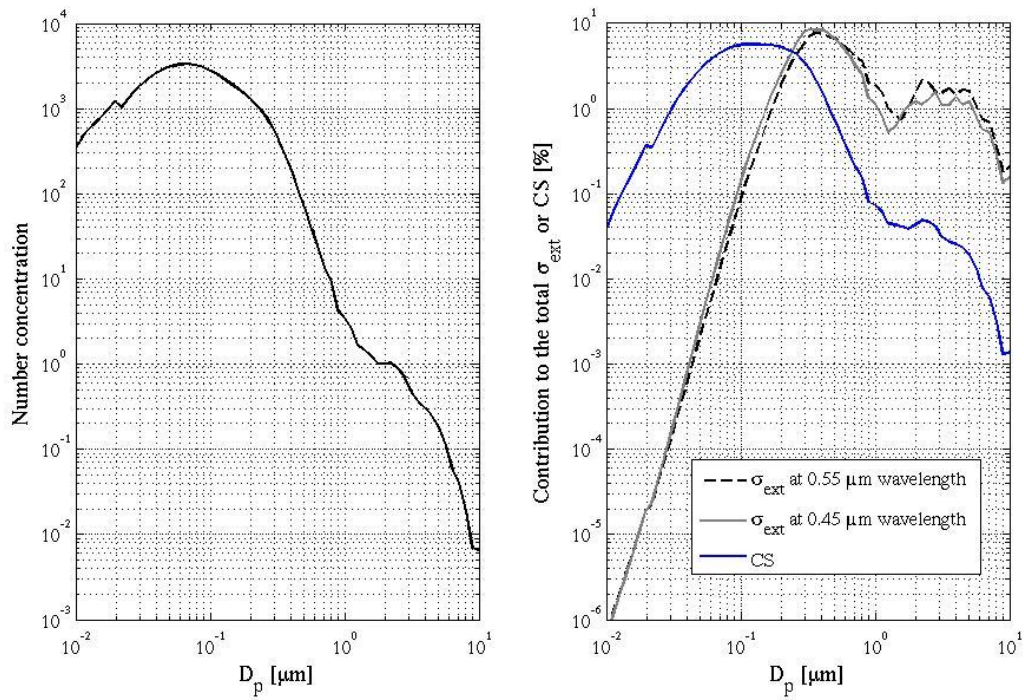


3

4 Figure 1. The study area and locations of the in situ measurement stations; BOT = Botsalano,
5 MAR = Marikana, WEL = Welgegend, and ELA = Elandsfontein.

6

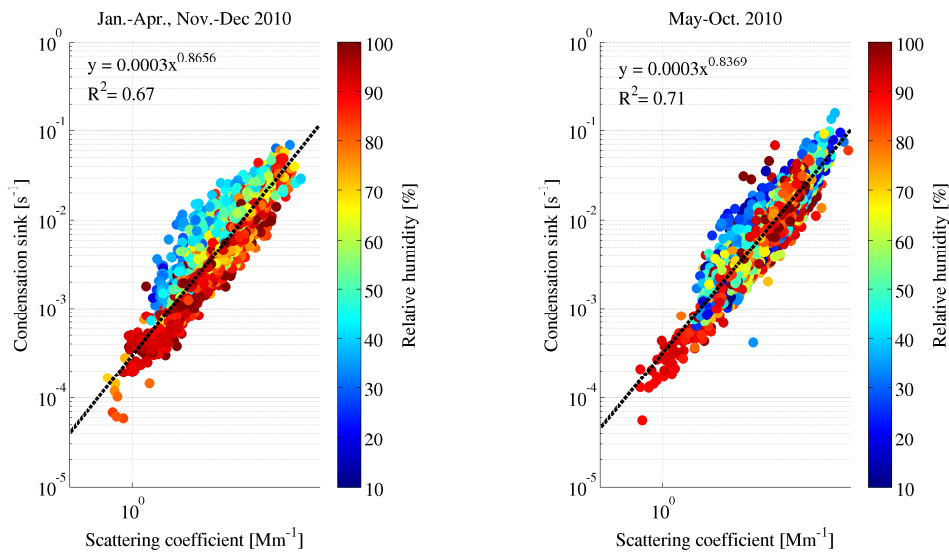
1



2

3 Figure 2. The sensitivity of CS and aerosol extinction coefficient to different particle sizes. In
4 the left panel is shown the aerosol size distribution that is used to calculate CS and σ_{ext} is
5 calculated for two wavelengths (0.55 and 0.45 μm) assuming spherical particles with a
6 refractive index of $m=1.48+0.001i$. In the right panel is shown the contribution of each
7 particle size to the total CS and σ_{ext} . The σ_{ext} is calculated for two wavelengths (0.55 and
8 0.45 μm) assuming spherical particles with a refractive index of $m=1.48+0.001i$.

9

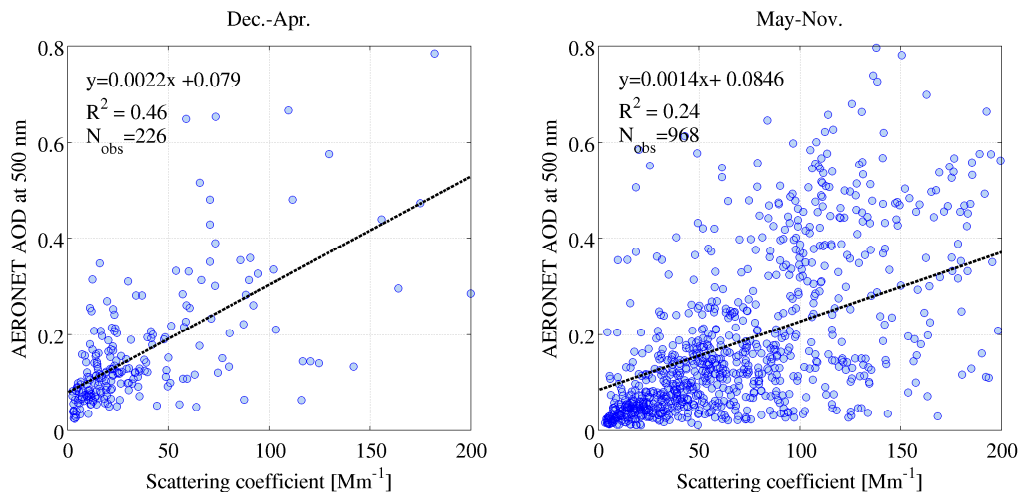


1

2 Figure 3. Comparison between condensation sinks derived from particle size distributions, as
 3 described in the text, and nephelometer scattering coefficients measured at Elandsfontein
 4 station in 2010 for the warm (Jan-Apr., Nov.-Dec), and the cold (May-Oct.) seasons. CS has
 5 been corrected to the ambient relative humidity but the scattering coefficient was measured
 6 from dry particles. The data are colour-coded according to ambient relative humidity (RH)
 7 and the strong influence of RH on the relation between CS and scattering coefficient is
 8 evident.

9

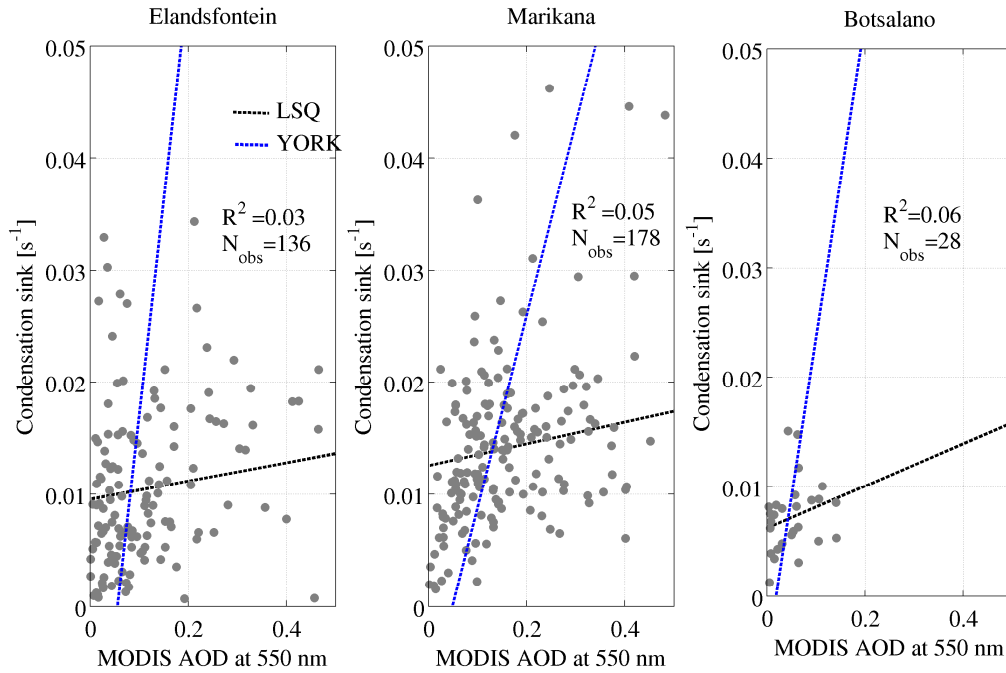
1



2

3 Figure 4. Comparison between AOD at 500nm available from AERONET (see text) and in
4 situ scattering coefficients measured at the Elandsfontein station. The AOD is the column
5 integrated value of aerosol extinction (scattering + absorption) obtained from sunphotometer
6 measurements. The in situ scattering coefficient is measured with a nephelometer.

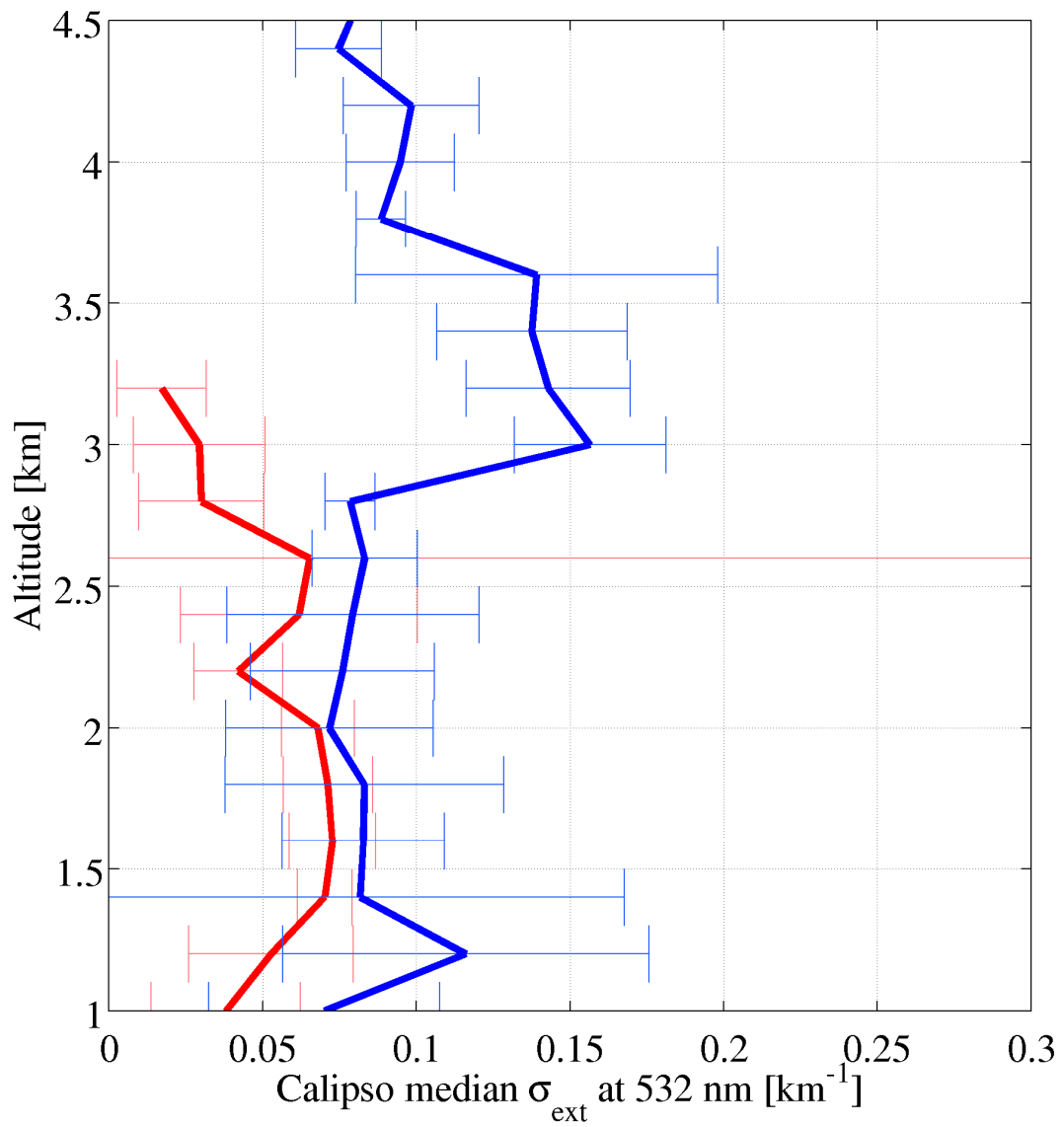
7



2

3 Figure 5. Comparison between MODIS AOD and in situ CS. The MODIS AOD values are
 4 spatial averages calculated from the observations within 3 km distance from the measurement
 5 station, whereas the CS values are one hour averages (13:00-14:00 LT). The black lines
 6 represent the slope from least squares linear fitting (LSQ). The blue lines represent the fitting
 7 method where the uncertainties related to CS and AOD values have been taken into account
 8 (YORK, York et al. 2004). The uncertainty for CS was set to 10 %, and for AOD to 0.05+15%
 9 (Levy et al., 2013).

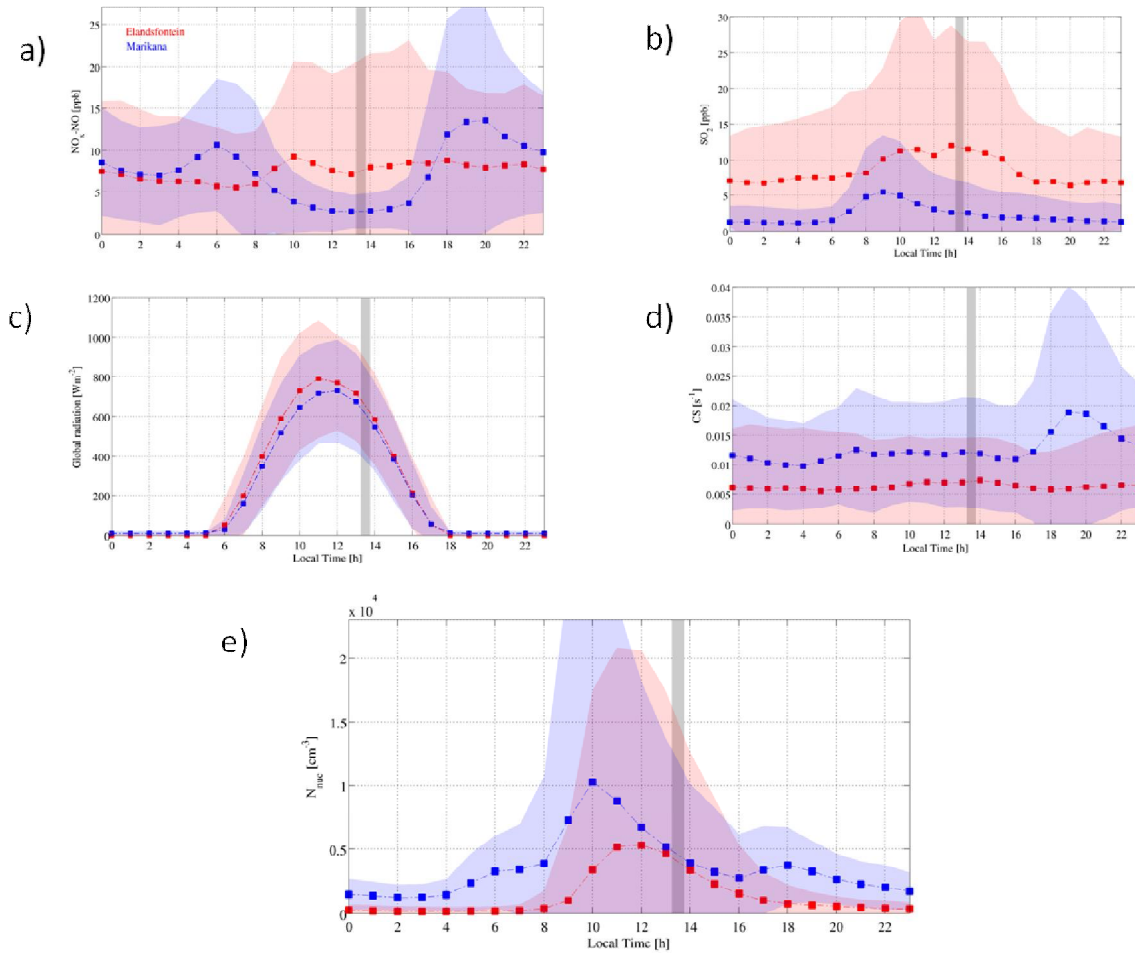
10



1

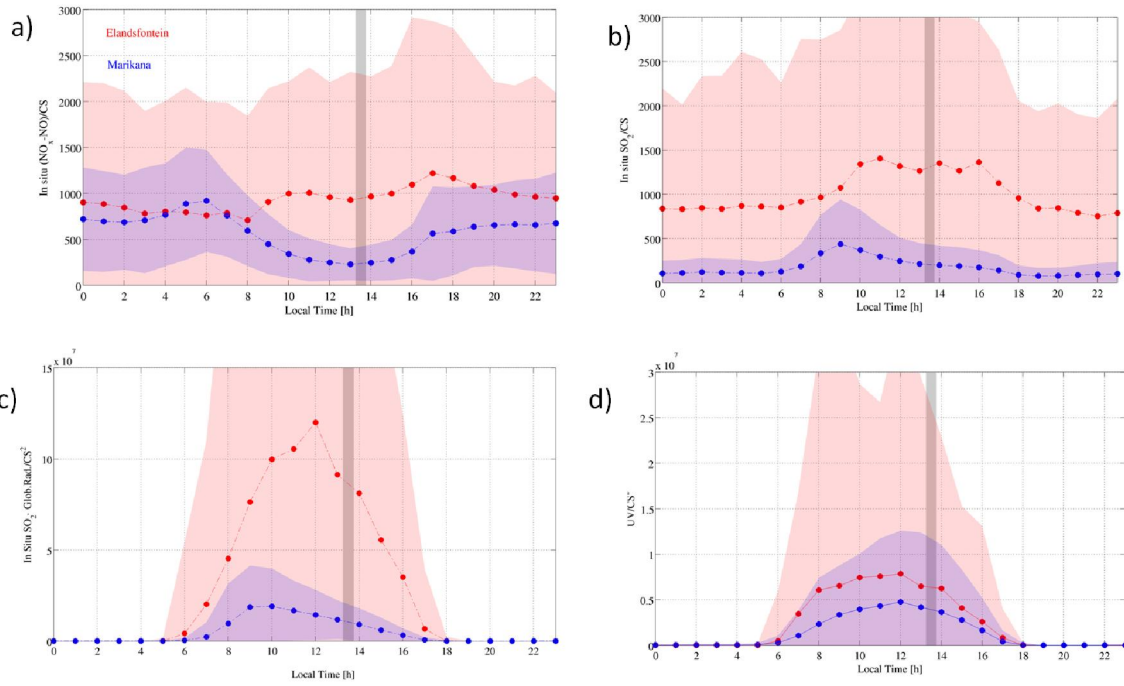
2 Figure 6. Median CALIPSO extinction profiles for days when MODIS AOD > 0.15 (blue)
 3 and AOD ≤ 0.15 (red). The CALIPSO profiles are collected within 50 km radius from the
 4 Marikana station. The horizontal bars represent the interquartile ranges.

5



1

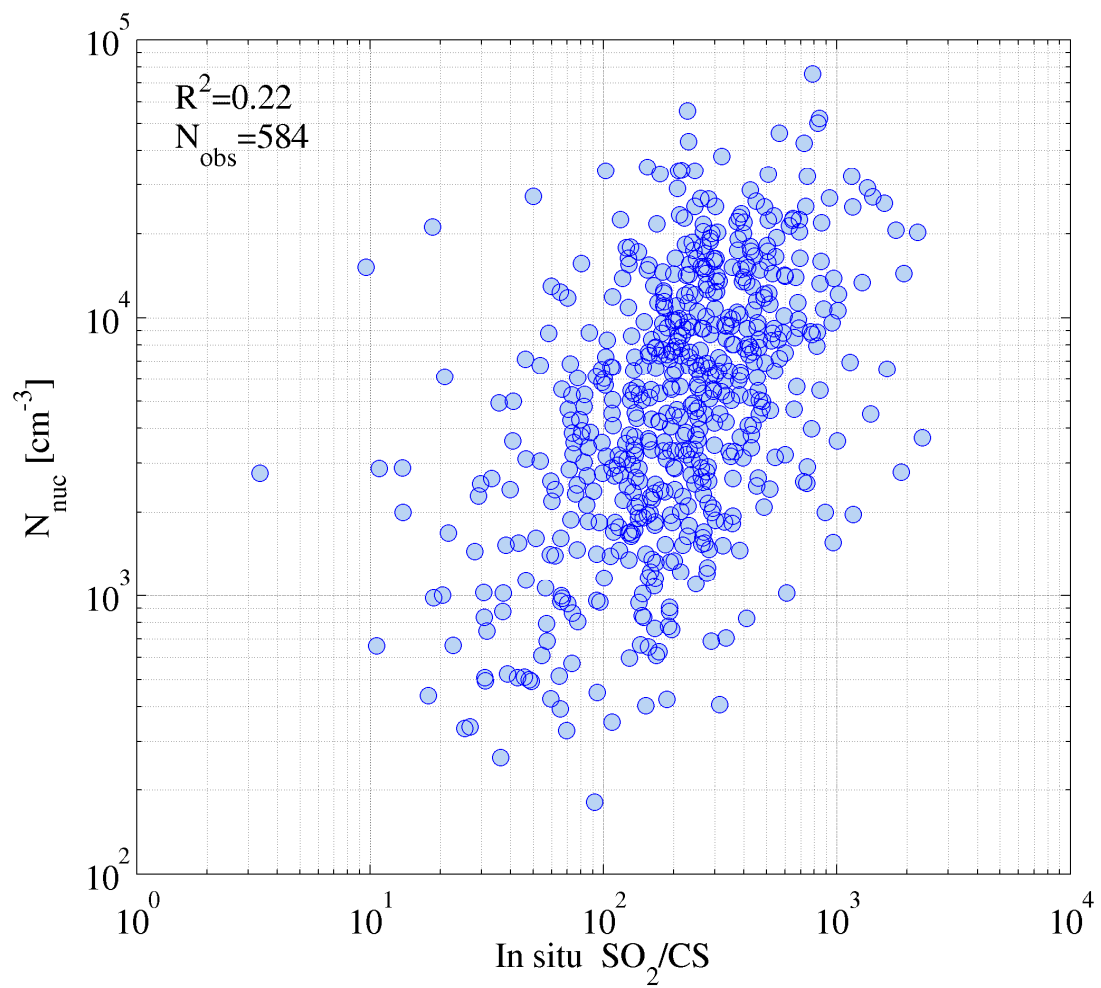
2 Figure 7. Diurnal variation of a) $\text{NO}_x\text{-NO}$, b) SO_2 , c) global radiation, d) CS, and e) N_{nuc} at
 3 Elandsfontein (red) and Marikana (blue) stations. The grey columns represent the time
 4 window for the satellite overpass. The blue and red shading denote the 75th and 25th
 5 percentile. It is noted that CS at Elandsfontein is defined with particles $D_p < 10\mu\text{m}$, and at
 6 Marikana with particles $D_p < 1\mu\text{m}$. N_{nuc} at Marikana represents particles $D_p < 30\text{ nm}$ while at
 7 Elandsfontein N_{nuc} represents particles $D_p 10\text{-}30\text{ nm}$.



1

2 Fig 8. Diurnal variation of the proxies calculated using in situ data at Elandsfontein (red) and
 3 at Marikana (blue) stations. The red and blue shaded areas denote the 75th and 25th percentile
 4 ranges. The grey column represents the time of the satellite overpass.

5

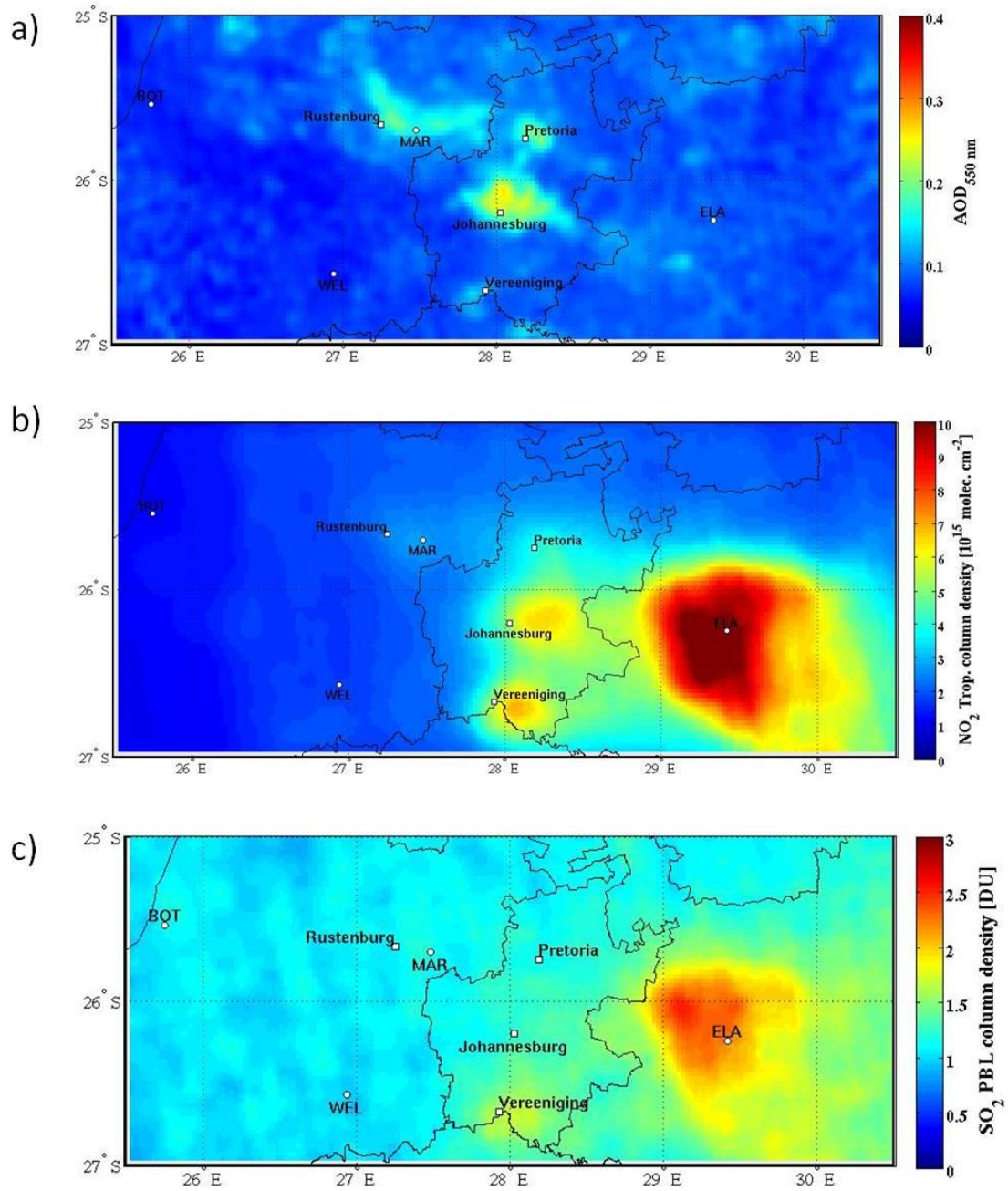


1

2 Fig. 9. Correlation between nucleation mode number concentration and SO_2/CS proxy
3 calculated using in situ data at Marikana measurement station at the time of the satellite
4 overpass (13-14 LT).

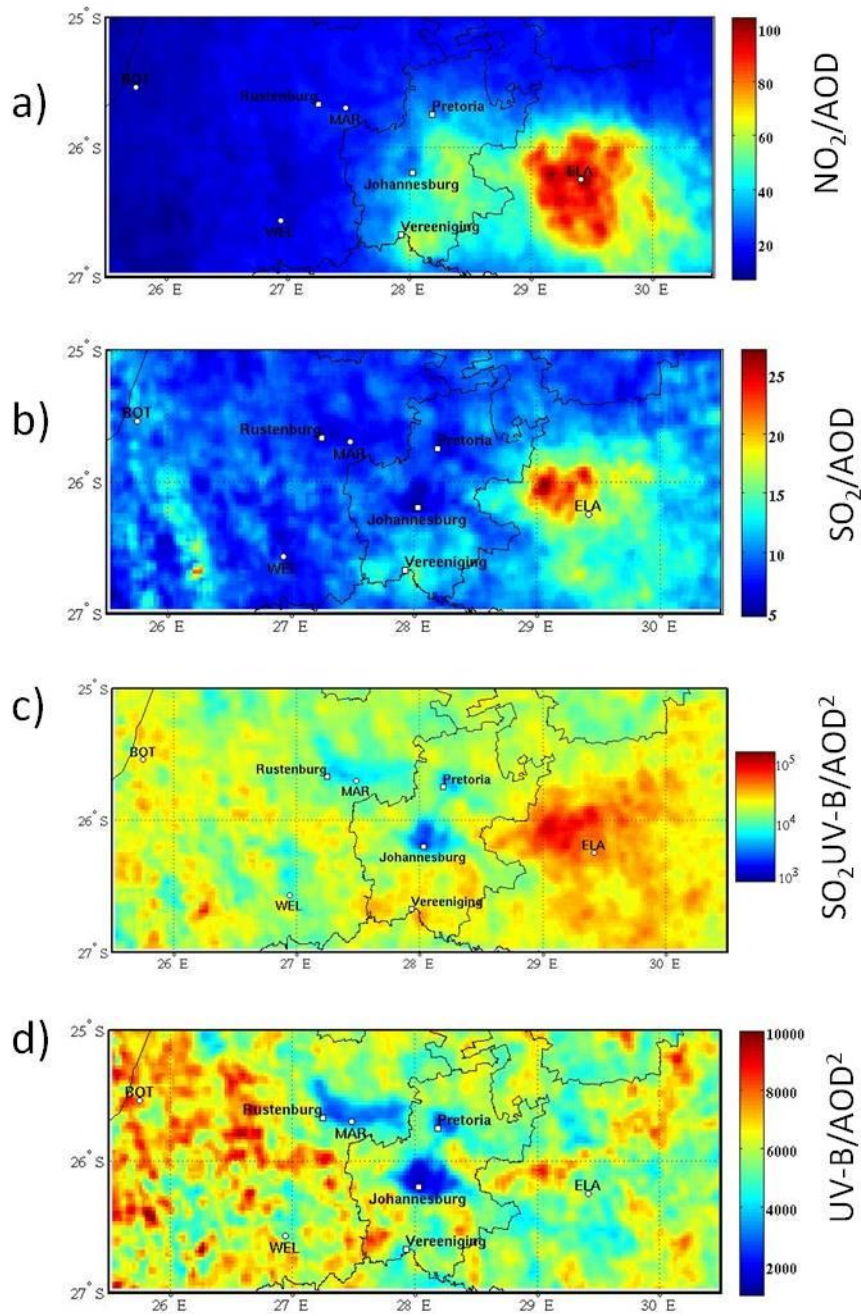
5

1
2

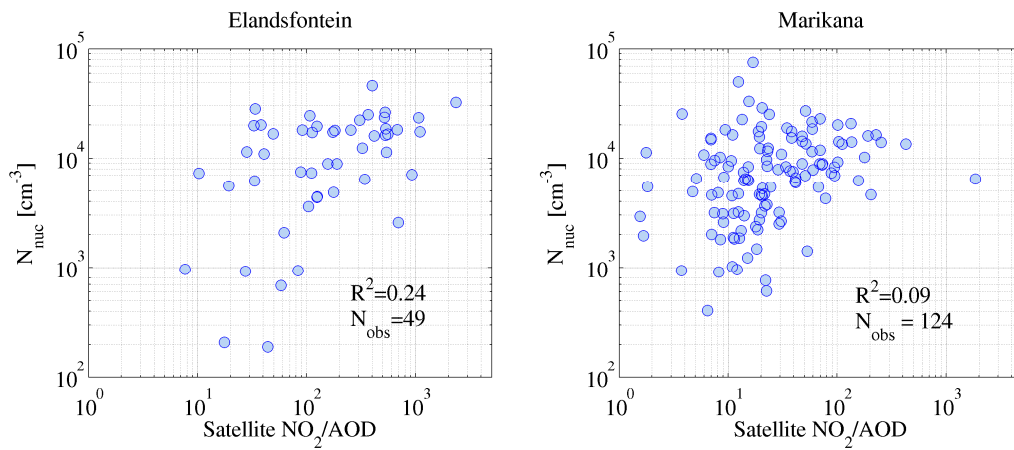


3
4
5
6
7
8
9

Figure 10. MODIS AOD (a) , OMI NO₂ (b) and SO₂ (c) column density medians for a four year period from Jan. 2007 to Dec. 2010. The locations of the in situ measurement stations (ELA= Elandsfontein, MAR=Marikana, BOT=Botsalano, and WEL=Welgegund) are marked with white dots.



1
 2 Fig. 11. Spatial pattern of proxy medians for 2007-2010 calculated using satellite data. The
 3 proxies are a) NO_2/AOD , b) SO_2/AOD , c) $\text{SO}_2 \cdot \text{UV-B}/\text{AOD}^2$, and d) $\text{UV-B}/\text{AOD}^2$.



1
2
3
4
5
6
7
8

Figure 12. The comparison between the number concentration of nucleation mode particles and NO_2/AOD calculated from the satellite data at Marikana and at Elandsfontein stations. The number concentrations are one hour averages (13-14 LT) representative of the satellite overpass time. It is noted that at Elandsfontein N_{nuc} represents particles with D_p 10-30 nm, and at Marikana particles with $D_p < 30$ nm. N_{obs} denotes the number of coincident observations.